JP&M Engineering
Journal of Petroleum and Mining Engineering
http://jpme.journals.ekb.eg/

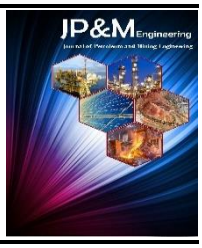

Effect of Post-Treatments on Corrosion and Electrochemical Properties of Anodized Al 2024-T3 Alloy

Wahba, A.[1,2] , Fattah, H. A.[2], Gouda, M. K.[2], Salman, S. A.[2] and Sadawy, M.M.[2]
[1]- Sianco - Egyptian Co. for Appliances and Maintenance, Cairo, Egypt.
[2]-Mining and Pet. Dept., Faculty of Engineering, Al-Azhar University, Nasr City, Cairo, Egypt.
*Corresponding author e-mail: Ahmed.wahba1900@gmail.com

Article Info

Received 25 Feb. 2023
Revised 2 Apr. 2023
Accepted 1 May 2023

Keywords

Aluminum, Anodizing, Sealing, Pitting

Abstract

Aluminum and its alloys are commonly used in engineering structures and components, particularly where lightweight and corrosion resistance is required. Nevertheless, it could be exhibited to corrosion under certain conditions in the atmosphere. So, surface treatments are needed to overcome this problem and achieve proper corrosion resistance. In this research, anodizing in sulfuric acid followed by sealing in hot water, ammonium acetate, and bichromate salt was performed on Al 2024-T3 alloy. X-ray diffraction (XRD), Scanning electron microscopy (SEM) / energy-dispersive X-ray spectroscopy unit (EDS), ,and a group of electrochemical technics were used to study morphology and the electrochemical behavior of the specimens. The results indicated that the sealing post-treatment decreased the cracks and sealed the pores on the anodic film surface to some extent based on the sealing method. When Al 2024-T3 alloy was sealed with bichromate, the surface became smoother and more crack-free than the other samples. Further, the corrosion properties showed a substantial improvement in the anti-corrosion properties of bichromate sealing compared to the anodized 2024 Al alloy with and without sealing in hot water and ammonium acetate solution.

Introduction

Aluminum and its alloys develop an aluminum oxide layer on their surfaces when exposed to air, which protects the metal's surface from corrosion to some extent. Moreover, the high thermal conductivity of aluminum makes it an excellent candidate for heating and cooling applications [1, 2]. Al 2024-T3 alloy is frequently employed in applications requiring high strength to weight ratio and good fatigue resistance, such as aircraft especially wing and fuselage structures which is under tension [3-5]. It has good workability. Depending upon its temper, the mechanical properties of 2024 aluminum can vary greatly. This alloy acquires its strengthening by combining Cu with Al and Mg forming strengthening precipitates, like Al2Cu and AlCuMg. These precipitates improve their mechanical performance. Unfortunately, introducing these phases with their distinct electrochemical characteristics into the Al-matrix resulted in localized corrosion and dissolution of Al-matrix in the corrosive environments [6]. For this reason, various surface treatment techniques are essential to enhance the anti-corrosion property of this alloy. Typical aluminum surface treatment techniques include anodizing, chemical conversion coating, plating, and cladding with a thin surface of high purity [7, 8]. One of the most prevalent surface treatments for aluminum and its alloys is anodizing. In this process, a decorative and protective film of aluminum oxide is developed on the aluminum surface using a direct current electrical supply. The most common aluminum anodizing processes use chromic acid, sulfuric acid, or oxalic acid [9]. Anodizing using Sulphuric acid is usually employed in industry to protect aluminum alloys against corrosion and wear [10, 11]. The anodic film contains an open pore-like structure; therefore, sealing the porous aluminum oxide layer can improve the anti-corrosion property and extend the anodic film's life [12].

The effect of sealing by phytic acid (PA) on sulfuric acid-anodized aluminum was investigated by Shuaixing Wang et al. [13]. The anodized aluminum was found to have a porous structure and low corrosion resistance. However, after sealing with phytic acid (PA), pores were sealed and a conversion film with a thickness of 3-4 m was formed, resulting in superior corrosion resistance compared to unsealed anodized aluminum.

Tian Lian-peng et al. [14] investigated the electrochemical behaviors of anodized aluminum sealed by Ce-Mo on 1070 aluminum alloy in NaCl solution. Their results showed that Ce-Mo sealing causes a formation of a uniform and compact surface on the anodic film. Moreover, an improvement in the corrosion resistance of anodic film was obtained as a result of the mutual effect of Ce and Mo. Choudhary et al. [15] examined the impact of the anodizing potential on the scratch behavior of aluminum alloy in oxalic acid. The results showed that rough and hard anodic aluminum oxide film with a

marginally greater amount of oxygen was formed at higher anodizing potentials. Lee et al. [16] applied sealing by immersing (several times) in a chromium oxide solution combined with heating. The electrochemical corrosion of the anodized layer was analyzed comparing with sealing by boiling water. They found that pores were completely sealed with γ-AlO(OH) (boehmite) after water sealing, and corrosion resistance was higher than in the anodized but unsealed sample. The effect of different sealing techniques on the corrosion of three aluminum alloys was examined by Zuo et al. [17]. Both boiling water and potassium dichromate-sealed films indicated superior corrosion resistance in the acidic solutions, whilst nickel fluoride-sealed films performed better in basic solutions. Moreover, stearic acid-sealed film was highly resistant to corrosion in both acidic and basic environments. Moonsu Kim et al. [18] applied sealing with NaAlO2 solution. Corrosion resistance, hardness, and sealing properties were found better compared to sealing by traditional methods. NaAlO2 sealing results in the deposition of a dense, hard layer of boehmite within the anodic film's pores, improving the film's chemical/mechanical properties. In this study, Al 2024-T3 alloy specimens were anodized in sulphuric acid followed by sealing in hot water, potassium bichromate solution and ammonium acetate solution. The potentiodynamic polarization results indicated that potassium bichromate sealing was drastically effective and exhibited excellent corrosion resistance compared to hot water sealing, ammonium acetate sealing and anodized (unsealed) Al 2024-T3 alloy.

Material of workpiece

An Al 2024-T3 alloy was studied in the current work with the exact chemical composition shown in table 1. All samples were prepared to be with the dimensions of (20 mm × 30 mm × 2 mm). Samples were grinded to 2000 grade emery paper, degreased in (0.5 M NaOH solution) for 10 min at 60 C°, then washed with distilled water following by hot air drying. The chemical analysis of the base alloy Al 2024-T3 were obtained from the Aluminum company of Egypt (Egyptalum).

Table 1. Show the composition of Al 2024-T3 alloy.

Element	Cu	Fe	Mg	Si	Ti	Zn	Al
%Weight	3.81	0.5	1.21	0.3	0.5	0.14	balance

Anodizing and Sealing

Anodizing was performed in Helwan Military Aviation Factory. The sealing was done in the laboratory of the department of Petroleum and Mining Engineering, Al-Azhar University. The samples were subjected to etching in alkaline solution (1 M NaOH) for 10 min at 50 C° and washed with distilled water, then introduced to the anodizing cell. Anodizing was performed in a solution containing 1.3 M H2SO4, 0.1 M oxalic acid, and 0.1 M potassium-sodium tartrate. The anodizing was achieved using a power supply with 20 V applied potential for 30 min. at ambient temperature. After that, the anodized specimens were sealed in different electrolytes, namely: hot water, (50 g/l ammonium acetate solution) and (50 g/l potassium bichromate solution) at a temperature of 90 C° for 30 minutes.

Table 2. anodizing and sealing processing parameters

Process	Processing parameters
Anodizing	(1.3 M H_2SO_4) + (0.1 M oxalic acid) + (0.1 M potassium- sodium tartrate), 20 V applied potential for 30 min. at ambient temperature.
Boiling water sealing	Deionized water, 90 C°, 30 min.
Ammonium acetate sealing	$C_2H_7NO_2$ ($CH_3COO\text{-}NH^{4+}$) 50 $g{\cdot}L^{-1}$, 90 C°, 30 min.
Potassium bichromate sealing	K_2CrO_7 - 50 $g{\cdot}L^{-1}$, 90 C°, 30 min.

Corrosion and surface characterization

The surface exposed to the electro chemical tests was with the area 10 mm × 10 mm. All electrochemical tests were made in a (3.5% NaCl) solution using three electrodes cell to characterize the corrosion properties as shown in Fig. 1. Working electrode was the sample of Al alloy, while (Pt coil), and (Ag/AgCl/saturated KCl) were counter and reference electrodes respectively. 2 Hours open-circuit potential (OCP) was performed. The Tafel plots were acquired by scanning the potential with the rate of (0.5 mV/s) in the positive direction. Cyclic polarization plots were conducted by moving the potential from -100 mV vs. Ecor to more noble potential using rate of 0.5 mV/s. The potential was moved in the opposed direction once the anodic current density value was 0.10 A/cm2. The surface morphologies, chemical composition, and phase structure of the samples were examined by X-ray diffraction, scanning electron microscopy, and energy-dispersive X-ray spectroscopy.

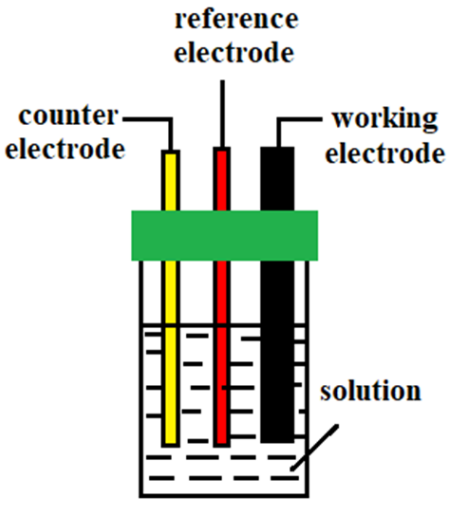

Figure 1 Schematic diagram showing the three-electrode cell

 DOI: 10.21608/jpme.2023.195590.1155

Results and discussion

Surface characterization

Fig. 2 and 3 show SEM images of anodized alloy before and after sealing in three different solutions. Clearly, the anodized sample Fig. 2(a) gives intense cavities and pores resulted from the selective dissolution of intermetallic precipitates throughout the anodizing process. The surface morphology of the hot water sealed samples of the anodized layer shown in Fig. 3(a) is not significantly distinct from the anodized sample shown in Fig. 2(a). This is consistent with similar results obtained by Lee et l. [16]. Conversely, Fig. 3(c and e) show that ammonium acetate and potassium bichromate possess the ability to close many pores in the porous skeleton of the anodic layer for Al 2024-T3 alloy.

Open circuit potential

The open circuit potentials (OCP) of sealed and unsealed samples in 3.5 wt.% solution is shown in Fig. 5. It is clear that all samples shift slowly to more positive values with an increment of the immersion time due to blocking some pores by hydration products [20, 21]. However, Fig. 5 shows that the OCP of all sealed samples give OCP higher than the unsealed sample. Depending on the type of sealing, the bichromate sealing sample exhibits a more positive value compared to the other samples. This behavior could be a result of the refined crystal structure of the hydration products, which prevents more cracks and protects against penetrating into the substrate Fig. 3(e). On the other hand, the hot sealed water sample exhibits the lowest potential compared with the other sealed samples due to unblocking some pores in the sealed film Fig. 3(a)

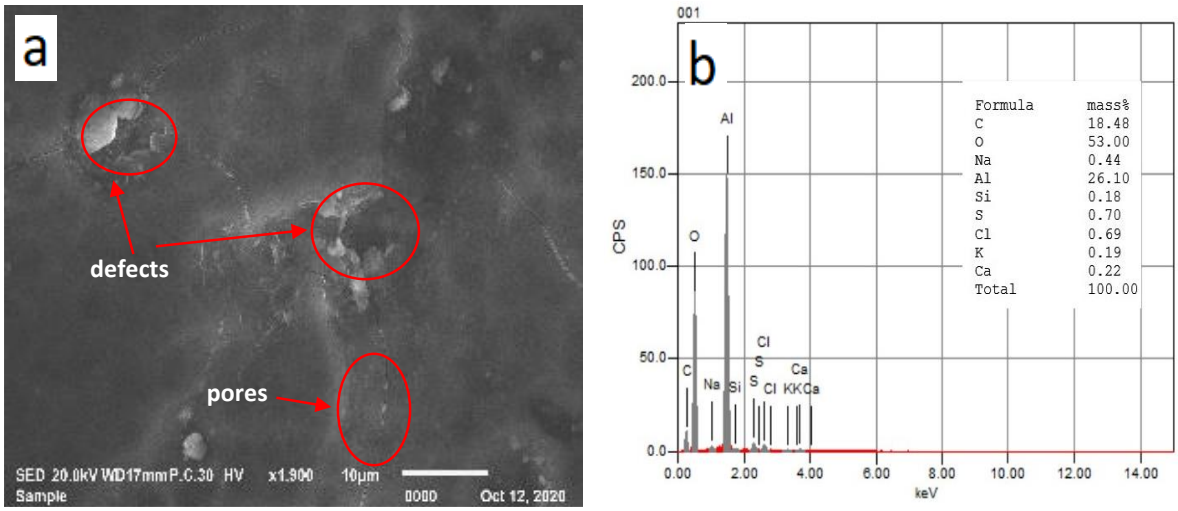

Figure 2 (a,b) SEM and EDS images of anodized 2024 Al alloy before sealing

Fig. 2 and 3 also show the EDS analysis related to each sample's film. The resultant peaks suggested that the anodizing Fig. 2 (b), the hot water sealing Fig. 3(b), and the ammonium acetate Fig. 3(d) films include Al, O, C, S, Ca, and Si with different ratios. While the outcomes reveal that bichromate sealing film Fig. 3(f) contains the same elements plus K and Cr.

The X-ray diffraction

The X-ray diffraction patterns of the anodized samples without sealing and after sealing in hot water, ammonium acetate solution, and potassium bichromate solution are shown in Fig. 4. The high-intensity peaks related to aluminum and aluminum oxide are detected for all samples. The absence of other detectable peaks, such as chromium oxide, is probably due to their low volume fractions. Similar outcomes were obtained by Korda and hidyat [19]. Nevertheless, the EDS spectrum confirms the existence of chromium in the alloy sealed with potassium bichromate, as shown in Fig. 3(f).

Potentiodynamic polarization

The potentiodynamic polarization curves of sealed and unsealed samples after immersion for 30 min in 3.5 wt.% solutions are shown in Fig. 6. Oxygen reduction reactions are the cathodic reactions as shown in Eq. (1):

$$O_2 + 2H_2O + 4e^- \rightarrow 4OH^- \qquad (1)$$

Notably, the cathodic current density of the anodized sample exhibits the greatest value compared with the other sealing samples. This behavior is attributed to the increment of the defects in the passive film of the anodized sample, causing the oxygen vacancy density to increase, hence, the oxygen reduction rate increases. The cathodic reactions are reduced because sealing films act as physical obstacles in the midst of substrates and the corrosive ions, as indicated by the sealed samples values of the cathodic current densities.

 DOI: 10.21608/jpme.2023.195590.1155

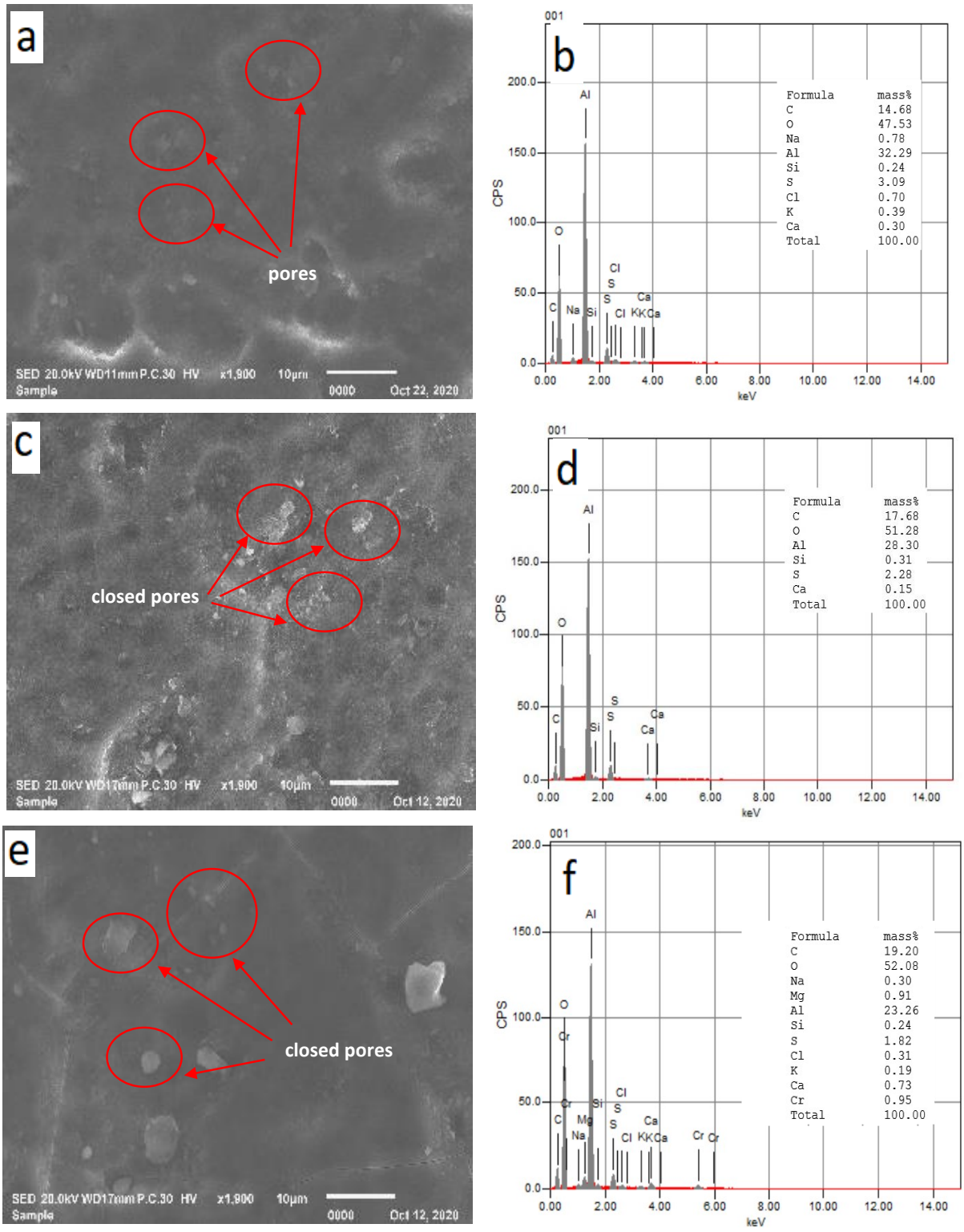

Figure 3 SEM and EDS images of anodized 2024 Al alloy after sealing in hot water (a,b), after sealing with ammonium acetate (c,d), and after sealing with bichromate solution (e,f)

In contrary, Fig. 6 reveals that the anodized sample has the greatest anodic current density owing to the dissolution of Al, Mg, and Cu from the matrix in accordance with the equations (2- 4) [22]:

$$Al \rightarrow Al^{+3} + 3e^{-} \quad (2)$$

$$Mg \rightarrow Mg^{+2} + 2e^{-} \quad (3)$$

$$Cu \rightarrow Cu^{+2} + 2e^{-} \quad (4)$$

 DOI: 10.21608/jpme.2023.195590.1155

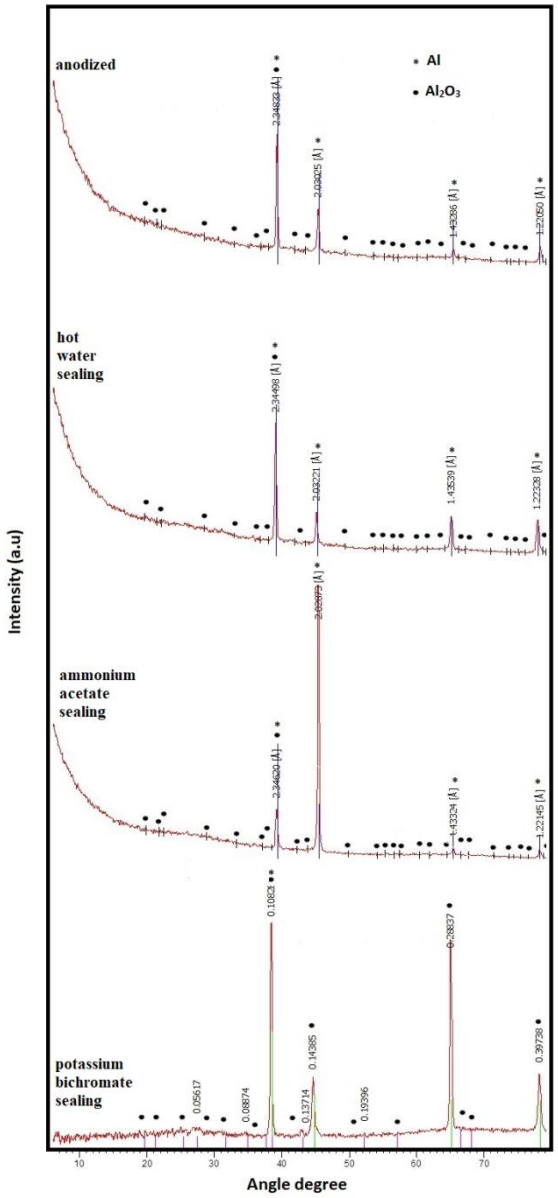

Figure 4 XRD patterns of anodized 2024 Al alloy without sealing and after sealing in hot water, ammonium acetate and potassium bichromate solutions.

The sealing samples give a notable reduction in the anodic current density compared with the unsealed sample due to the closing of some pores, which act as a barrier between the substrate and the corrosive ions. The outcomes of the corrosion potentials (Ecorr), corrosion current densities (Icorr), corrosion rates (Vcorr), and both cathodic and anodic Tafel slopes (βc and βa) are listed in table 3. It can be observed that the corrosion potential of the anodized sample is (-679 mV), exhibiting a more active trend due to dropping the pH of the electrolyte, which results from a formation of more metal hydroxide, while the bichromate exhibits the highest Ecorr value (-611 mV). On the other hand, the corrosion current density was (85.5 µA/cm2), (15 µA/cm2), (2.4 µA/cm2) and (0.21 µA/cm2) for anodized, hot water, ammonium acetate and bichromate sealing samples respectively.

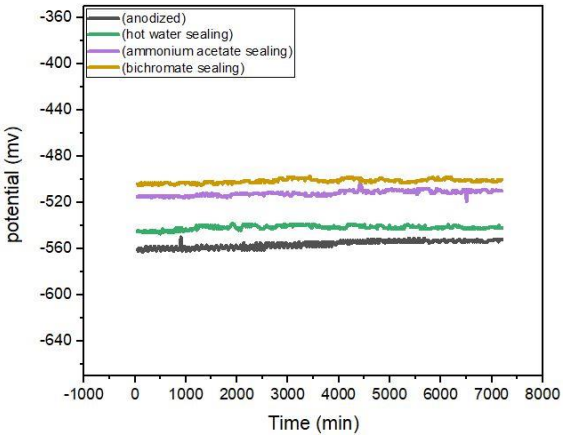

Figure 5 OCP of the anodized alloy without sealing and after sealing with different methods after immersion in the 3.5 wt% NaCl solution for 2 h

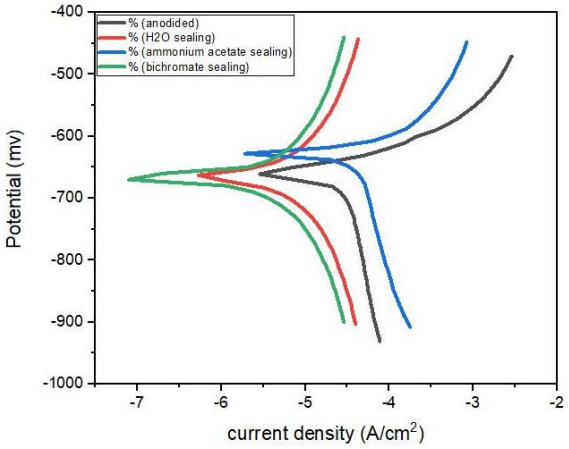

Figure 6 Tafel plots of the anodized alloy without sealing and after sealing with different methods after immersion in the 3.5 wt% NaCl solution for 30 min

Table 3. Electrochemical parameters obtained from Fig. 6

Sample type	E_{cor} (mV)	i_{cor} (µ-A/cm²)	B_c (mV/dec)	β_a (mV/dec)
Anodized	-679±11	85.5±0.13	282±20	330±13
Hot water sealed	-666±13	15 ±0.22	217±12	358±11
Ammonium acetate sealed	-639±10	2.4±0.02	275±10	312±12
Bichromate sealed	-611± 12	0.21±0.01	280±11	328±14

 DOI: 10.21608/jpme.2023.195590.1155

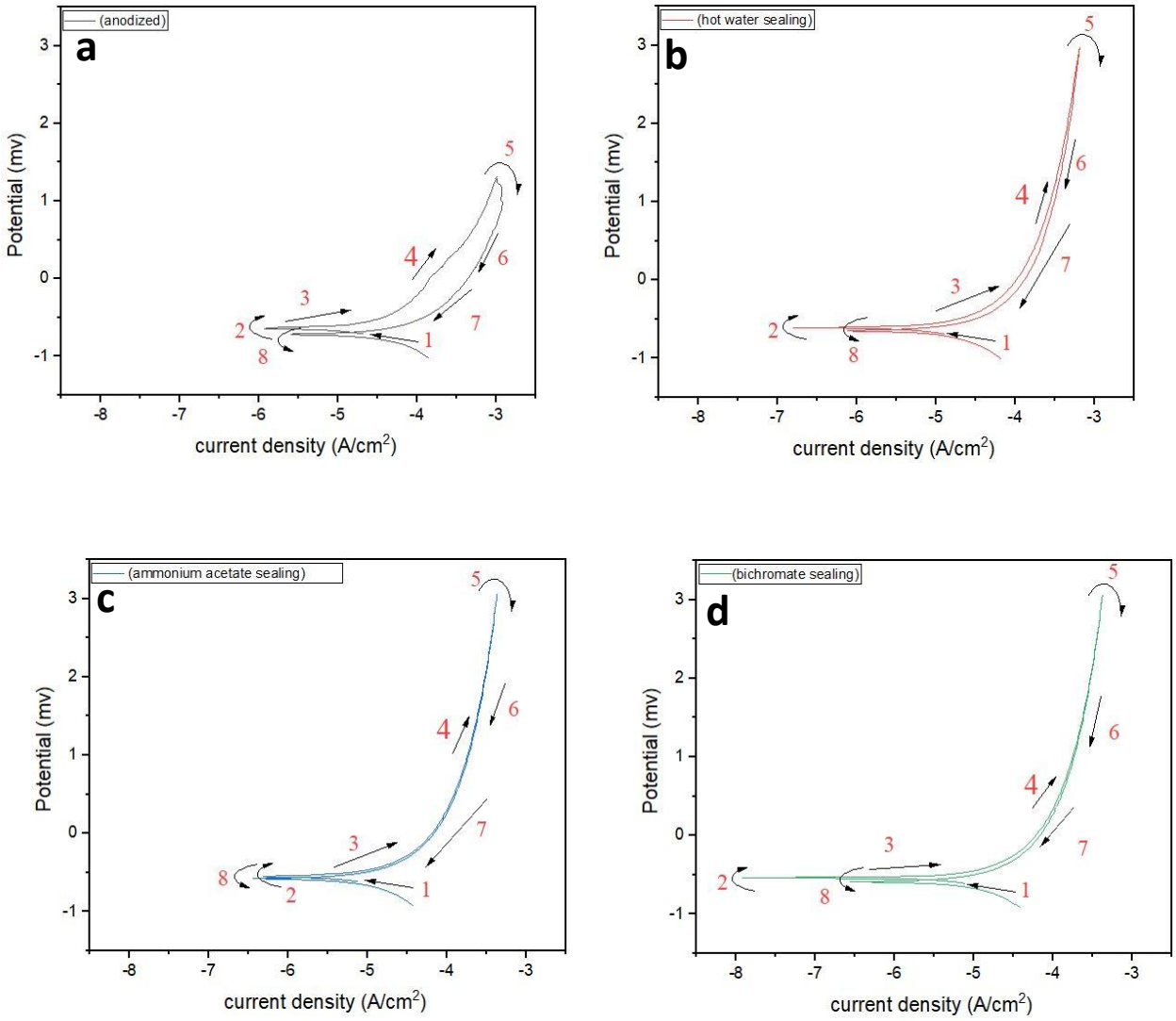

Figure 7 Cyclic polarization plots of the anodized alloy without sealing and after sealing with different methods after immersion in the 3.5 wt% NaCl solution for 30 min.

Table 4. Electrochemical parameters obtained from Fig. 7

Sample Type	E_{pit} (mV)	i_{pit} ($A \cdot cm^{-2}$)	E_{pass} (mV)	i_{pass} ($A \cdot cm^{-2}$)	Passive zone (mV)
Anodized	1280±21	$(10.23\pm0.30)\times10^{-4}$	-324±9	$(75.85\pm1.10)\times10^{-6}$	1604±32
Hot water sealed	2946±99	$(6.46\pm 0.10)\times10^{-4}$	-222±6	$(66.07\pm0.90)\times10^{-6}$	3168±63
Ammonium acetate sealed	3046±111	$(4.26\pm0.09)\times10^{-4}$	-177±4	$(47.86\pm0.87)\times10^{-6}$	3223±77
Bichromate sealed	3055±113	$(4.21\pm0.08)\times10^{-4}$	-190±5	$(38.90\pm0.76)\times10^{-6}$	3245±78

 DOI: 10.21608/jpme.2023.195590.1155

Cyclic polarization

Pitting susceptibility and passivity of sealed and unsealed 2024-T3 in NaCl solution were investigated using the cyclic polarization technique. Fig. 7 represents the cyclic polarization results for all samples after the immersion in 3.5wt.% NaCl solution, for 30 min. It can be obviously noted that all samples have analogous shape, showing an explicit corrosion potential zone followed by a passive zone.

of sealed and unsealed samples after cyclic polarization tests are presented in Fig. 8. Evidently, all samples show signs of pitting corrosion. Still, both width and shape of the pits rely significantly on the sealing method. Fig. 8 (a) displays that the anodized sample suffers from a large, corroded size. The hot water sealing Fig. 8 (b) also suffers from a large pit size but is lower than the anodized sample. On the other hand, the ammonium acetate and bichromate sealing samples Fig. 8 (c,d) suffer from low-size pits

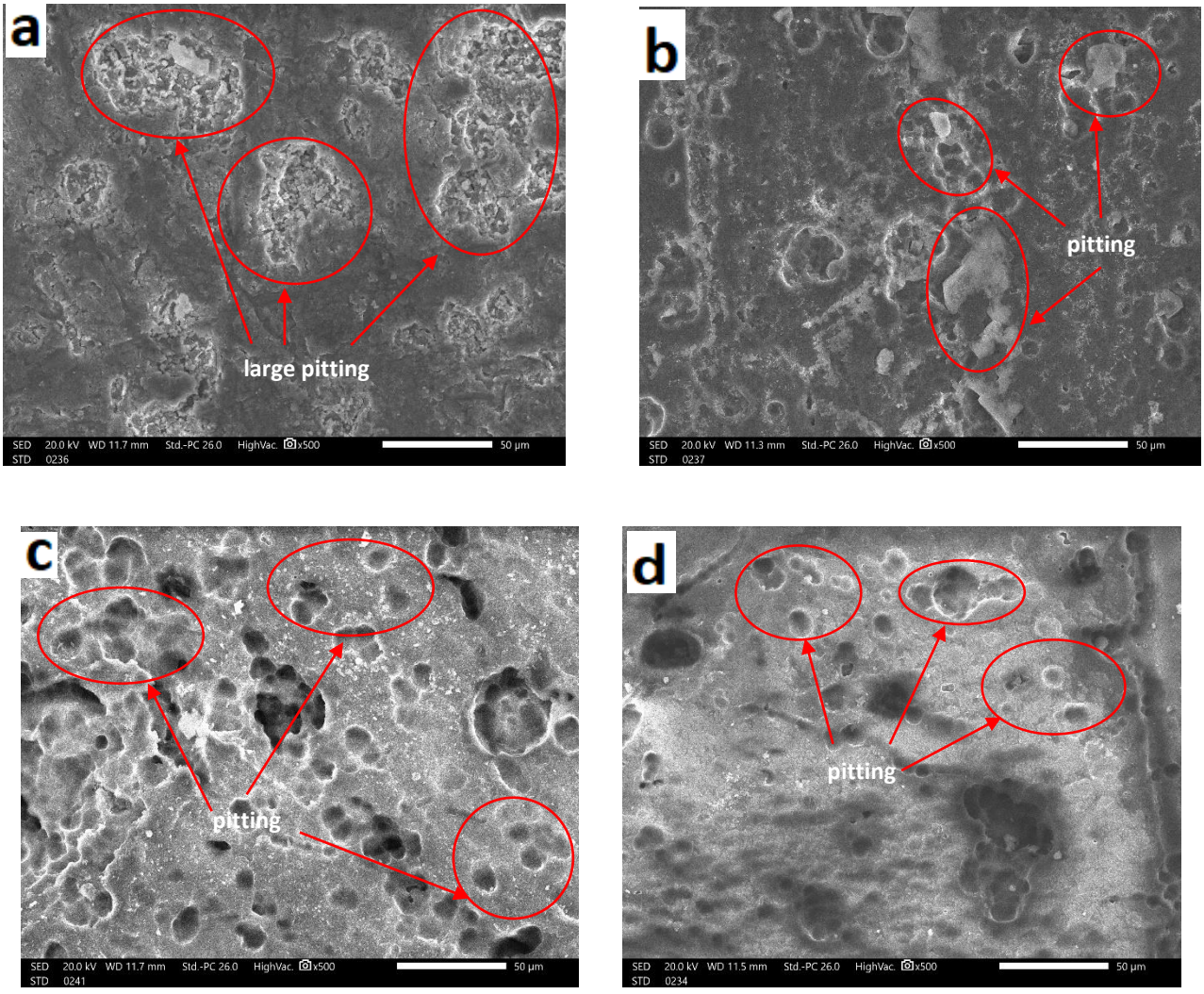

Figure 8 The SEM morphologies of sealed and unsealed samples after cyclic polarization tests.

However, the anodized sample gives the lowest passive zone of about (1604mV) due to the presence of more opening pores and defects in the anodized film. Further, the outcomes reveal that the values of the passive zones for sealing samples are similar to each other. Table 4 shows the electrochemical parameter values extracted from cyclic polarization curves for all samples in 3.5wt.% NaCl solution. The results discloses that the passivation region of bichromate sealing is nearly (3245 mV), which is larger than all samples. This behaviour is ascribed to forming of the Cr_2O_3 passive film, which has a more dense and protective physical barrier than Al_2O_3 or $Al(OH)_3$ [19]. Further, Table 4 indicates that pitting potential varies from (1280mV), (2946mV), (3046mV), and (3055mV), depending on the sealing method. The SEM morphologies

Conclusion

Anodizing of 2024 aluminum alloy was performed in a solution constituted from (1.3 M H_2SO_4) + (0.1 M Oxalic acid) + (0.1 M Potassium- Sodium tartrate). Sealing with hot water, ammonium acetate, and bichromate solutions was applied after anodizing. The aluminum phases were the major constituent of the anodic film formed on 2024 Al alloy with and without sealing. The sealing post-treatment decreased the cracks and sealed the pores on the anodic film surface. When sealed with bichromate, the surface becomes smoother and crack-free than the other samples. The corrosion properties show a substantial improvement in the anti-corrosion properties of bichromate sealing compared to the anodized 2024 Al

alloy with and without sealing in hot water and ammonium acetate solution.

Conflicts of interest

There are no conflicts to declare

References

[1] Polmear, I., et al., The Light Metals, in Light Alloys (Fifth Edition), I. Polmear, et al., Editors. 2017, Butterworth-Heinemann: Boston. p. 1-29.

[2] Mallick, P.K., Overview, in Materials, Design and Manufacturing for Lightweight Vehicles, P.K. Mallick, Editor. 2010, Woodhead Publishing. p. 1-32.

[3] Davis, J.R., Corrosion of aluminum and aluminum alloys. 1999, United States: Materials Park, OH (United States); ASM International.

[4] Sankaran, K.K. and R.S. Mishra, Chapter 4 - Aluminum Alloys, in Metallurgy and Design of Alloys with Hierarchical Microstructures, K.K. Sankaran and R.S. Mishra, Editors. 2017, Elsevier. p. 57-176.

[5] Donatus, U., et al., Corrosion pathways in aluminium alloys. Transactions of Nonferrous Metals Society of China, 2017. 27(1): p. 55-62.

[6] Ghosh, K., M. Hilal, and B. Sagnik, Corrosion behavior of 2024 Al-Cu-Mg alloy of various tempers. Transactions of Nonferrous Metals Society of China, 2013. 23(11): p. 3215-3227.

[7] Starke, E.A. and J.T. Staley, Application of modern aluminium alloys to aircraft, in Fundamentals of Aluminium Metallurgy, R. Lumley, Editor. 2011, Woodhead Publishing. p. 747-783.

[8] Rambabu, P., et al., Aluminium alloys for aerospace applications, in Aerospace materials and material technologies. 2017, Springer. p. 29-52.

[9] Wernick, S., R. Pinner, and P. Sheasby, The Surface Treatment and Finishing of Aluminum and Its Alloys. Vol. 1 and 2.(Book). 1987, United States: ASM International. 1987.

[10] Ebihara, K., Structure and density of anodic oxyde films formed on aluminium in sulfuric acid solutions. Journal of The Surface Finishing Society of Japan 34, 1983. 34: p. 548-553.

[11] Wood, G. and J. O'sullivan, The anodizing of aluminium in sulphate solutions. Electrochimica acta, 1970. 15(12): p. 1865-1876.

[12] Vlot, A. and J.W. Gunnink, Fibre Metal Laminates: An Introduction. 2011: Springer Netherlands.

[13] Wang, S., et al., Sealing of anodized aluminum with phytic acid solution. Surface and Coatings Technology, 2016. 286: p. 155-164.

[14] Tian, L.-P., et al., Electrochemical behaviors of anodic alumina sealed by Ce-Mo in NaCl solutions. Transactions of Nonferrous Metals Society of China, 2006. 16(5): p. 1178-1183.

[15] Choudhary, R.K., et al., Scratch behavior of aluminum anodized in oxalic acid: effect of anodizing potential. Surface and Coatings Technology, 2015. 283: p. 135-147.

[16] Lee, J., et al., Cr2O3 sealing of anodized aluminum alloy by heat treatment. Surface and Coatings Technology, 2014. 243: p. 34-38.

[17] Zuo, Y., P.-H. Zhao, and J.-M. Zhao, The influences of sealing methods on corrosion behavior of anodized aluminum alloys in NaCl solutions. Surface and Coatings Technology, 2003. 166(2-3): p. 237-242.

[18] Kim, M., H. Yoo, and J. Choi, Non-nickel-based sealing of anodic porous aluminum oxide in NaAlO2. Surface and Coatings Technology, 2017. 310: p. 106-112.

[19] Korda, A.A. and d.R. Hidayat. Effect of CrO3 Sealing Time on Anodized A12024-T3. in Journal of Physics: Conference Series. 2016. IOP Publishing.

[20] Xiao, K., et al., Galvanic corrosion of magnesium alloy and aluminum alloy by kelvin probe. Journal of Wuhan University of Technology-Mater. Sci. Ed., 2016. 31: p. 204-210.

[21] Xu, J., et al., Effect of Al alloying on cavitation erosion behavior of TaSi2 nanocrystalline coatings. Ultrasonics Sonochemistry, 2019. 59: p. 104742.

[22] Fayed, S.M., et al., Corrosion inhibition characteristics of multilayer Si-DLC, phosphating and anodizing coatings deposited on 2024 Al alloy: A comparative study. Diamond and Related Materials, 2021. 117: p. 108460.